Bi-specific Aptamers Mediating Tumor Cell Lysis[S]

Achim Boltz[‡§], **Birgit Piater**[‡§], **Lars Toleikis**[§], **Ralf Guenther**[§], **Harald Kolmar**[‡], and **Bjoern Hock**[§1]

From the [‡]Clemens-Schoepf-Institute for Organic Chemistry and Biochemistry, Technical University Darmstadt, D-64289 Darmstadt and the [§]Protein Engineering and Antibody Technologies Department, Merck Serono, Merck KGaA, D-64293 Darmstadt, Germany

Antibody-dependent cellular cytotoxicity plays a pivotal role in antibody-based tumor therapies and is based on the recruitment of natural killer cells to antibody-bound tumor cells via binding of the Fcγ receptor III (CD16). Here we describe the generation of chimeric DNA aptamers that simultaneously bind to CD16α and c-Met, a receptor that is overexpressed in many tumors. By application of the systematic evolution of ligands by exponential enrichment (SELEX) method, CD16α specific DNA aptamers were isolated that bound with high specificity and affinity (91 pM–195 nM) to their respective recombinant and cellularly expressed target proteins. Two optimized CD16α specific aptamers were coupled to each of two c-Met specific aptamers using different linkers. Bi-specific aptamers retained suitable binding properties and displayed simultaneous binding to both antigens. Moreover, they mediated cellular cytotoxicity dependent on aptamer and effector cell concentration. Displacement of a bi-specific aptamer from CD16α by competing antibody 3G8 reduced cytotoxicity and confirmed the proposed mode of action. These results represent the first gain of a tumor-effective function of two distinct oligonucleotides by linkage into a bi-specific aptamer mediating cellular cytotoxicity.

Aptamers are structured single-stranded oligonucleotides that can bind to a large variety of targets with high affinity and specificity (1, 2). Aptamers can be isolated by an *in vitro* selection and an evolution process referred to as systematic evolution of ligands by exponential enrichment (SELEX)[2] (3, 4). Because aptamers have the capacity to inhibit protein-protein interactions with potencies similar to those observed with antibodies, aptamers can also trigger inhibition signals, *e.g.* by blocking receptor multimerization, and consequently act as therapeutic antagonists. Reversely, bi- and multivalent aptamers can activate co-stimulatory receptors, *e.g.* to enhance T cell reactivity (5, 6). Finally, aptamers can be applied in ligand-based targeted therapies to specifically deliver cytotoxic payloads (7, 8) or siRNA (9) to tumor cells. Monoclonal antibodies serve as established and successful tumor therapeutics. However, naturally bivalent antibody formats comprise the risks of immunogenicity (10) and undesired activation by receptor dimerization (11). Development of monovalent therapeutic antibodies is elaborate and time-intensive (MetMAb (12)). Although antibodies exceed aptamers with proof as therapeutic molecules, high stability, and good pharmacokinetics, the potential advantages of aptamers are a rapid optimization, cost-effective and uniform synthesis, and a high probability of an absence of immunogenicity (5, 13). Approval of Macugen (pegaptanib sodium (14)) as the first therapeutic aptamer in 2007 as well as promising approaches in preclinical development and clinical trials (15, 16) only a few years after inception of the technology indicate aptamers as a promising new class of targeted therapeutics.

Antibody-dependent cellular cytotoxicity (ADCC (17)) originating from the interaction of Fc fragments of antibodies with Fcγ receptors (FcγR) on natural killer (NK) cells plays a pivotal role in antibody-based tumor therapies (18, 19). NK cells are critical to host defense against invading organisms (20), are important for suppressing tumor metastasis and outgrowth (21), and can additionally stimulate components of the adaptive immune system to eliminate tumors (19, 22). ADCC, phagocytosis, and clearance of immune complexes by NK cells (23) are mediated by the intermediate affinity Fc receptor FcγRIIIα or CD16α (24). CD16α is expressed by NK cells, δγ-T cells, monocytes, and macrophages. The low affinity isoform FcγRIIIβ (CD16β) is highly related to CD16α and expressed on human neutrophils and eosinophils. Both isoforms can be proteolytically cleaved off cells (25, 26), but the prevalent soluble isoform is sCD16β (27). The CD16α polymorphism Phe-158 to Val-158 enhances its affinity for IgG1 and is associated with improved clinical outcome in tumor patients treated with therapeutical antibodies (28, 29). Several studies revealed ADCC as one major mode of action of antibody-based therapeutics (30, 31) and stimulated more interest in how to mobilize, expand, and activate NK cells in humans (32). So far, antibody effector functions such as recruitment of NK cells (33–35) or cytotoxic T cells (36) were successfully transferred to therapeutic, scFv-based bi-specific antibody strategies but could not be exploited in an aptamer format. Enabling NK cell recruitment to tumors by CD16α specific aptamers could combine the advantages of this molecule format with the potency of the tumor-effective function of ADCC (Fig. 1).

Receptor tyrosine kinases (RTKs) are key regulators of critical cellular processes such as cell growth, differentiation, and tissue repair, but aberrant expression can contribute to the development and progression of cancer (37). In this study, the

---

[1] To whom correspondence should be addressed: Merck KGaA, Frankfurter Str. 250, D-64293 Darmstadt, Germany. Tel.: 49-6151-72-2722; Fax: 49-6151-72-3447; E-mail: Bjoern.Hock@merck.de.

[2] The abbreviations used are: SELEX, systematic evolution of ligands by exponential enrichment; ADCC, antibody- or aptamer-dependent cellular cytotoxicity; bsA, bi-specific aptamer; FcγR, Fcγ receptor; CD16, FcγRIII; NK cells, natural killer cells; scFv, single-chain Fv fragment; PBMC, peripheral blood mononuclear cell.
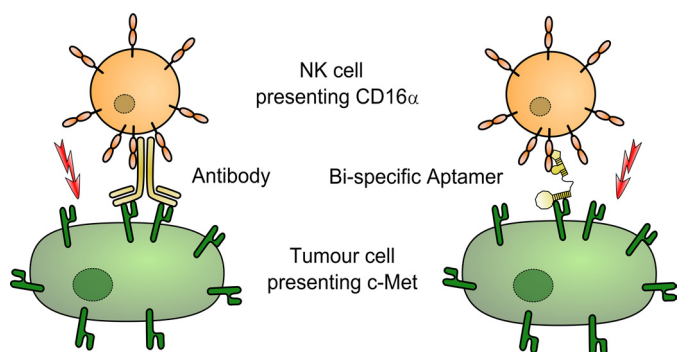
FIGURE 1. **Concept of bi-specific aptamers mediating tumor cell lysis.** Bi-specific aptamers mimic ADCC by recruitment of natural killer cells via FcγRIIIα (CD16α) to c-Met-overexpressing tumor cells.

receptor tyrosine kinase hepatocyte growth factor receptor (HGF-R or c-Met) was used as a tumor-associated antigen for specific targeting of tumor cells. c-Met is a multidomain receptor tyrosine kinase expressed on cells of epithelial origin (38, 39) and is essential for embryonic development (40) and wound healing. Aberrant c-Met signaling due to dysregulation of the receptor or overexpression of the natural ligand hepatocyte growth factor induces several biological responses that collectively give rise to invasive growth (37, 41, 42).

Specific recruitment of NK cells to c-Met-overexpressing tumors by a bi-specific aptamer simultaneously binding to c-Met and CD16α could induce ADCC and represent a suitable starting concept for the development of stable, nucleotide-based tumor therapeutics. High affinities to both CD16α allo-forms Val-158 and Phe-158 in addition to high specificity to CD16α over the CD16β isoform could induce ADCC independent of allelic status or soluble CD16β decoy proteins. In addition, the monovalent tumor antigen binding architecture of the aptamers would enable inhibitory effects while *per se* excluding undesired c-Met activation. We herein present the first gain of a tumor-effective function of two distinct oligonucleotide entities by linkage into a bi-specific aptamer mediating tumor cell lysis.

EXPERIMENTAL PROCEDURES

Aptamers and Target Proteins—Aptamers up to 100 bp in length were synthesized and PAGE-purified by Eurofins MWG Operon (Ebersberg, Germany), and longer and PEG-linked oligonucleotides were from Integrated DNA Technologies (Leuven, Belgium). Target proteins CD16α-6His, CD16β-10His, and c-Met-Fc were purchased at R&D Systems, and Fc-CD16α Val-158 and Phe-158 fusion proteins were kindly provided by Angela Lim (EMD Serono).

Aptamer Selection on Recombinant Protein—An ssDNA oligonucleotide library containing a 40-base random sequence flanked by primer regions on either end was used as a starting point for aptamer selection. The library sequence was 5′-GG-AGGGAAAAGTTATCAGGC-(N)$_{40}$-GATTAGTTTTGGAGTACTCGCTCC-3′, the forward primer was 5′-GGAGGGAAAAGTTATCAGGC-3′, and the reverse primer was 5′-GGAGCGAGTACTCCAAAACTAAT-riboC-3′ (43). Aptamer amplification and precipitation were performed as described (81). Usage of a 3′-terminal ribo-dCTP reverse primer

enabled alkaline-induced antisense strand break followed by Tris-borate-EDTA-PAGE strand separation (biostep gels). The respective ssDNA band was extracted with a scalpel, and aptamers were eluted for 18 h at 37 °C in 300 mM sodium acetate (Merck), 20 mM EDTA (Invitrogen) buffer, precipitated, and reconstituted in DPBS (Invitrogen).

Aptamer selection was based on the separation of target protein with bound aptamers on 0.5 M KOH-pretreated nitrocellulose filters (Whatman), whereas unbound aptamers were removed by washing. Selections were performed for 12 consecutive rounds at 37 °C in a 100-μl final volume DPBS for 1 h to obtain aptamers for use under physiological conditions. The first selection rounds were carried out with 1.6 μM aptamer library, 1 μM target protein, and 500-μl DPBS washing volume. From round 2 on, 1 μM pools were used with decreasing protein and increasing tRNA competitor concentrations (up to 1 mg/ml), two 1000-μl washing steps, negative filter selections (to remove filter binding sequences), and adequate counterselections at equal concentrations. Aptamers were eluted with preheated 7 M urea, 100 mM sodium acetate, 3 mM EDTA elution buffer. Precipitation, PCR amplification, reverse strand break, and PAGE purification (as above) yielded an enriched aptamer pool for further SELEX cycles. Pools of several rounds were cloned with a TOPO-TA cloning kit (Invitrogen) before sequencing of 96 clones per round (Eurofins MWG Operon). Sequences were grouped into aptamer families of 90% sequence identity using DNA Star SeqMan software. Structure prediction was obtained by the mfold software (44) set to salt concentrations as in DPBS and 37 °C.

Cell SELEX—Cell SELEX was initiated with 1 μM pools of CD16α DNA filter SELEX rounds 3 and 5 as pre-enriched starting libraries using alternating 2×10^7 recombinant CD16α Val-158- or Phe-158-positive Jurkat cells in a cross-selection, with decreasing cell amounts in later rounds. Counterselection was carried out from round 2 using CD16α-negative Jurkat E6.1 cells. Selections were performed at 37 °C, 300 rpm for 30 min in 200 μl of binding buffer (0.05% BSA in DPBS), and two 1-ml washing steps were implemented by centrifugation. Cell-bound aptamers were purified by phenol/chloroform extraction, and then amplified and analyzed as described above.

Dot Blot Affinity Determination—Affinities were determined essentially as described (81). Briefly, 5 fmol of radiolabeled aptamers were incubated with protein dilution series for 30 min at 37 °C in 30 μl of dot blot buffer (0.1 mg/ml tRNA, 0.1 mg/ml BSA, DPBS), and then aptamer-protein complexes were captured on a nitrocellulose filter (Schleicher and Schuell; pretreated as before), whereas unbound aptamers were immobilized on a PVDF Hybond P membrane (GE Healthcare; pretreated with methanol, water, and DPBS). Radioactivity was quantified using a Storm PhosphorImager and ImageQuant software (GE Healthcare). The percentage of aptamer bound was calculated using the formula: % of aptamer bound = 100 × (cpm of nitrocellulose/cpm of nitrocellulose + cpm of PVDF), and the background signal (aptamer bound to buffer only) was subtracted. Binding curves were plotted in Microsoft Excel, and K_D values were calculated by non-linear fitting using XL fit (IDBS, Surrey, UK).

Flow Cytometry—Cellular binding was determined using a FACScan cytometer and CellQuest software (BD Biosciences) as described (45). Briefly, 100 pmol of 3′-biotinylated aptamer or 10 μg of biotinylated reference antibody were used, and 1.5×10^4 events were detected via streptavidin-R-phycoerythrin conjugate (Sigma-Aldrich). All samples were incubated at 21 °C and 300 rpm due to temperature-dependent affinities of some aptamers (supplemental Fig. S7). Propidium iodide (Invitrogen) enabled dead cell exclusion by appropriate gating.

Bi-specific Aptamers and Linker Length Estimation—All aptamers were synthesized as one oligonucleotide chain and PAGE-purified. The nucleotide-to-nucleotide distance was averaged from the single-stranded portions of Protein Data Bank (PDB) entries 1HUT and 1OOA with PyMOL software (Schrödinger, LLC) to be 7 Å. Maximal putative linker lengths were calculated using this estimation.

Electrophoretic Motility Shift Assay—5 pmol of aptamer were incubated with 40 pmol of CD16α-6His and/or 15 pmol of c-Met-Fc in 10 μl of DPBS for 30 min at 37 °C. 2 μl of 6× DNA gel loading buffer (Novagen) were added, and the total volume was run on a water-cooled 4–20% Tris-borate-EDTA gel (biostep) followed by ethidium bromide staining (Invitrogen) and detection with a trans-illuminator (Alpha Innotech).

Serum Stability—10 pmol of gel-purified, radiolabeled oligonucleotides were incubated in PBS-buffered 90% FBS (Invitrogen), freshly prepared murine serum, or DPBS (Invitrogen) and analyzed as described (55). Half-life curve fitting was performed using the Origin software (OriginLab).

Cell Lines and Isolation of PBMC and NK Cells—Jurkat E6.1 (ATCC TIB 152) were cultured in RPMI 1640 + 2 mM glutamine, 1 mM sodium pyruvate, and 10% fetal calf serum (FCS) (all Invitrogen). 100 nM methotrexate (Sigma-Aldrich) was added to the culture medium of transfected Jurkat CD16α Val-158 or Phe-158 cells. GTL-16 cells were cultured in 10% FCS supplemented DMEM medium. MKN-45 cells (DMSZ ACC 409) were cultured as Jurkat cells but with 20% FCS, and EBC-1 cells (HSRRB JCRB0820) were cultured in minimal Eagle's medium (Sigma-Aldrich) with 2 mM glutamine and 10% FCS. All cells were kindly provided by Christa Burger, Merck Serono, and cultured at 37 °C and 5% CO_2, except for GTL-16 incubated at 10% CO_2. PBMC were isolated by Ficoll density gradient centrifugation from peripheral blood from healthy donors (at Merck, Darmstadt, Germany) using Lymphoprep tubes (Axis-Shield) following the manufacturer's protocol. NK cells were further enriched by MACS using an NK cell isolation kit (Miltenyi Biotec) following the manufacturer's instructions. All cells were used immediately after isolation.

ADCC Assay—ADCC assays were performed for 4 h at 37 °C and 5% CO_2 at least in triplicate in a GAPDH release aCella-TOX assay (Cell Technology) using 10^4 target cells and PBMCs. Aptamer dilutions in RPMI 1640 with 10% ultralow IgG FCS (both Invitrogen) were measured at a constant PBMC:target cell ratio of 80:1. For blocking experiments, the CLN0020-competing monoclonal antibody 3G8 (BioLegend) was added at a 20-fold molar excess. Enzyme solutions were added as suggested by the manufacturer, and bioluminescence was immediately measured on a VarioSkan Flash luminometer (Thermo Scientific). Mean values of all references were calculated using

Microsoft Excel, the "medium only" background signal was subtracted, and lysis was calculated using the formula

$$\% \text{ of specific lysis} = 100 \times \frac{SL - STCL - SECL}{ML - STCL} \quad \text{(Eq. 1)}$$

where SL = sample lysis; STCL = spontaneous target cell lysis; SECL = spontaneous effector cell lysis; and ML = maximal lysis.

RESULTS

Aptamer Selection and Characterization—SELEX to select CD16 specific DNA aptamers using recombinant human CD16α-6His and CD16α Val-158 or Phe-158 alloforms expressed on recombinant Jurkat cells yielded enriched pools in all selections (supplemental Figs. S1–S5). Pool sequencing revealed 29 enriched aptamer families (of >90% sequence identity in the randomized region), in parts unique to one selection but also found throughout all pools of later SELEX rounds (supplemental Fig. S5 and supplemental Table S1). CD16α specific aptamers bound with 6–429 nM affinities to recombinant CD16α, but not to the highly related isoform CD16β (Fig. 2, *A* and *C*, supplemental Fig. S6). However, specific cellular binding to CD16α on recombinant Jurkat or NK cells was only observed for CLN0020 and CLN0123. CD16α specificity was confirmed by flow cytometry in which both NK cells and recombinant CD16α-positive cells were bound, and no unspecific binding to CD16-negative Jurkat E6.1 cells could be observed (Fig. 2). CLN0123 showed lower CD16α affinity (193 nM, supplemental Figs. S6 and S8) and, as expected, only weak cellular binding (supplemental Fig. S8). Competition dot blots revealed that CLN0020 and CLN0123 bound in or near the Fc binding domain of CD16α, but bound to different epitopes (supplemental Fig. S11).

c-Met specific DNA aptamer sequences were isolated and characterized analogously to CD16α filter SELEX. CLN0003 and CLN0004 c-Met affinities (91 pM and 11 nM, respectively) were accompanied by specific cellular binding to c-Met-positive cell lines GTL-16, MKN-45, and EBC-1 (Fig. 2). Fc only as well as c-Met-negative Jurkat E6.1 cells were not bound (Fig. 2m *B*, *D*, and *E*). Biotinylated aptamers used for flow cytometry are shown in Fig. 3*C*, and selected aptamers are listed with sequence and affinities in Table 1.

Structure Prediction and Minimization—Using the mfold tool yielded a reasonable structure prediction for CLN0020 only (Fig. 3*A*), and the predicted 34-mer core sequence could be confirmed in dot blots to be essential. Removal of only base C20 resulted in a distinct affinity loss (Fig. 3*B*), whereas adjacent sequences were redundant (Fig. 3*C*). Other aptamers could be minimized individually (Fig. 3*C*). With information about core and putative linker sequences given, these four partly minimized sequences were used for the construction of bi-specific aptamers.

Bi-specific Aptamers—24 different bi-specific aptamers (bsA1–bsA32) were designed (Table 2 and supplemental sequence data), and they were all synthesized as one individual oligonucleotide chain. Differently minimized aptamers were used to screen for a suitable linker length while retain-
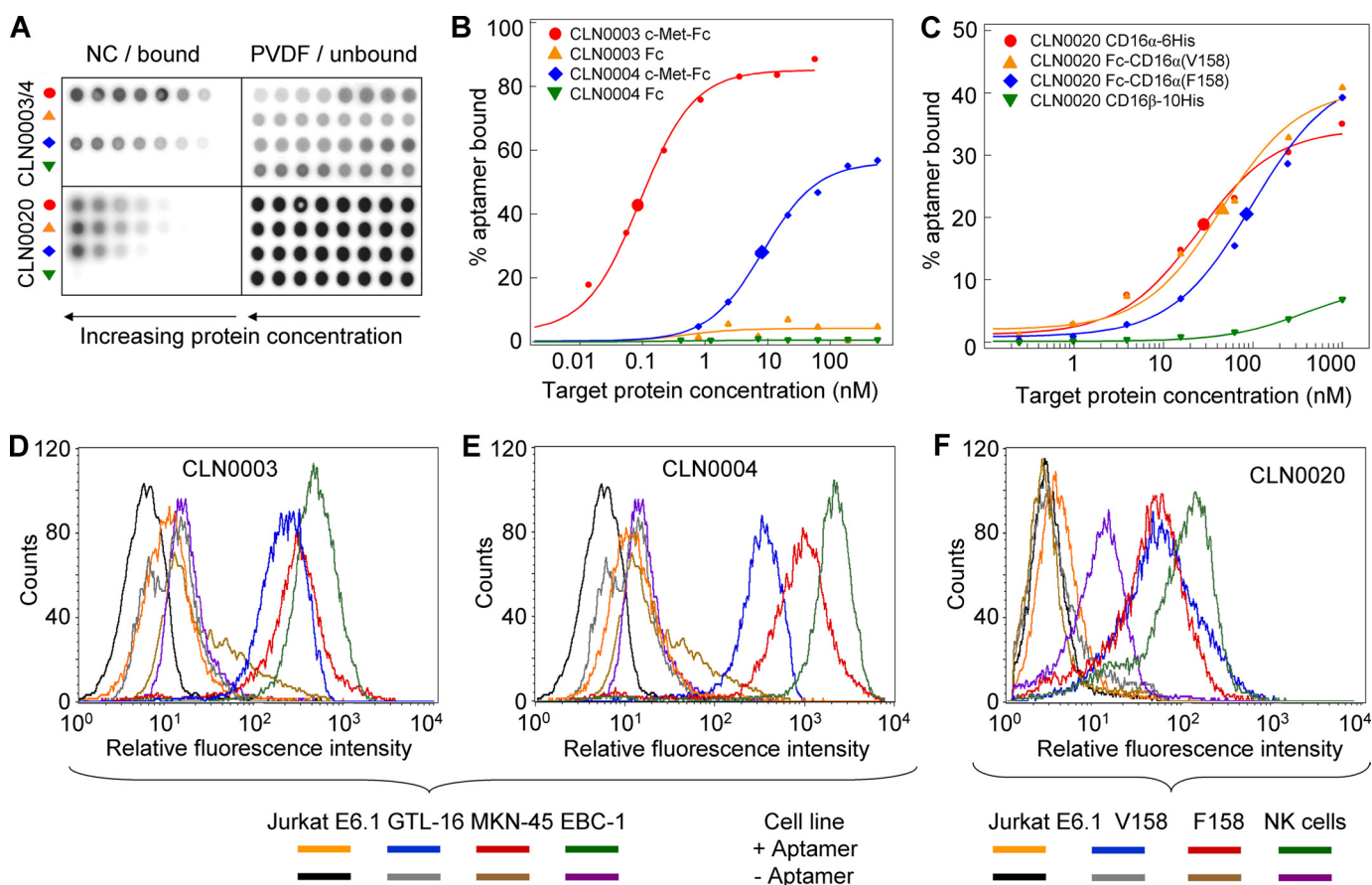
FIGURE 2. **Biochemical and cellular binding characterization of CD16α and c-Met specific aptamers.** *A*, representative dot blot raw data of three DNA aptamers CLN0003, CLN0004, and CLN0020. *NC*, nitrocellulose membrane readout; *PVDF*, polyvinylidene difluoride membrane readout. *B*, fitted binding curves for CLN0003 and CLN0004 to c-Met or Fc. *C*, fitted CLN0020 binding to both CD16α allotypes and minor binding to CD16β. *Enlarged symbols* represent calculated K_D values. *D*, FACS analysis of CLN0003 binding to c-Met-positive GTL-16, MKN-45, and EBC-1 cells as compared with c-Met-negative control Jurkat E6.1 cells. *E*, CLN0004 binding to Met-positive GTL-16, MKN-45, and EBC-1 cells as compared with Jurkat E6.1. *F*, CLN0020 binding to NK cells and to both alloforms of CD16α presented on recombinant Jurkat cells, in comparison with the parental, CD16-negative Jurkat E6.1 cell line.

TABLE 1

Selected DNA aptamers binding c-Met or CD16α (a complete list can be found in supplemental Table S2)

Aptamer	SELEX Target	Sequence[a]	K_D	n	Frequency in SELEX[b]
			nM		*%*
CLN0003	c-Met	TGGATGGTAGCTCGGTCGGGGTGGGTGGGTTGGCAAGTCT	0.09 ± 0.04	3	3
CLN0004	c-Met	GAGTGCGTAATGGTACGATTTGGGAAGTGGCTTGGGGTGG	11 ± 5	6	10
CLN0015	CD16	GGCAGAAGAAATATCGAAACCCAGAATGGTCGGCCAGGCG	24 ± 18	7	31
CLN0020	CD16	CACTGCGGGGGTCTATACGTGAGGAAGAAGTGGGCAGGTC	45 ± 28	10	4
CLN0021	CD16	GCAAGTATGAGCGCAGGAGTTAGGTCCCGTGGCGATGGGT	25 ± 19	5	40
CLN0023	CD16	GACGTTAAGCTAGCAGGTGTTAGGTCCCGTGGTGATGAAT	18 ± 14	5	2
CLN0030	CD16	TAAACCCCAAAACAGTGCAACTAGGTGTAGGTCCCGTGGT	6 ± 5	6	4
CLN0118	CD16	ACGGACTCGCAAAAGGTGGAACAGGAGTGGGGCCCCGCGGC	31 ± 20	2	27
CLN0123	CD16	AGAGGGGAGGGTCGGGTATCGGCGTGTTCGGGGGATCTGC	193 ± 29	4	2
CLN0126	CD16	GGCGTTGTCGGGCGCAGGTGTAGGCCTCGTGGTGGTGGGT	46 ± 11	2	6

[a] Aptamer families are shown without the flanking constant regions used for selection.
[b] Frequencies of most sequence families varied in several analyzed selection rounds; the highest respective frequency is stated.

ing high affinities, and several kinds of linker were applied: a 15-deoxyadenosine linker (46), up to 44 nucleotides as "original" linker derived from full-length sequences known to be not essential for binding, as well as short polyethylene glycol (PEG) chains (supplemental Table S3). Assuming that an optimal bsA linker should bridge approximately the distance spanning from complementarity-determining regions to the Fc binding domain in the hinge region of an antibody, this distance was estimated from measurement of PDB entry 1T83 (47) to be ~65 Å. Bi-specific aptamers were designed

with putative linker lengths of ~0–217 Å (Table 2 and supplemental Table S3).

Most bi-specific aptamers retained high affinities in dot blots similar to the respective parental clones, such as picomolar c-Met affinities of CLN0003-derived bsA17 (Table 2 and supplemental Fig. S12). CD16α affinities of bi-specific aptamers based on CLN0020 were 19–82 nM, whereas bsA15 showed 174 nM CD16α affinity similar to the parental aptamer CLN0123 (Table 2). Simultaneous binding to both target proteins was confirmed for bsA17 and bsA31 by electrophoretic

A

CLN0020

B

C

CLN0003	Truncated sequence	K_D (nM)
	GGAGGGAAAAGTTATCAGGCTGGATGGTAGCTCGGTCGGGGTGGGTGGGTTGGCAAGTCTGATTAGTTTTGGAGTACTCGCTCC ☆	0.09
	GGAGGGAAAAGTTATCAGGCTGGATGGTAGCTCGGTCGGGGTGGGTGGGTTGGCAAGTCTGATTAGTTTTGGAGTACTCGCTCC-B	0.25
	GAAAAGTTATCAGGCTGGATGGTAGCTCGGTCGGGGTGGGTGGGTTGGCAAGTCTGATTAGTTTTGGAGTACTCGCTCC	0.75
	AGTTATCAGGCTGGATGGTAGCTCGGTCGGGGTGGGTGGGTTGGCAAGTCTGATTAGTTTTGGAGTACTCGCTCC	9
	ATCAGGCTGGATGGTAGCTCGGTCGGGGTGGGTGGGTTGGCAAGTCTGATTAGTTTTGGAGTACTCGCTCC	12
	GGCTGGATGGTAGCTCGGTCGGGGTGGGTGGGTTGGCAAGTCTGATTAGTTTTGGAGTACTCGCTCC	49
	TGGATGGTAGCTCGGTCGGGGTGGGTGGGTTGGCAAGTCTGATTAGTTTTGGAGTACTCGCTCC	54
	GGAGGGAAAAGTTATCAGGCTGGATGGTAGCTCGGTCGGGGTGGGTGGGTTGGCAAGTCTGATTAGTTTTGGAGTACTC	0.65
	GGAGGGAAAAGTTATCAGGCTGGATGGTAGCTCGGTCGGGGTGGGTGGGTTGGCAAGTCT ☆	3
	TGGATGGTAGCTCGGTCGGGGTGGGTGGGTTGGCAAGTCT	52
CLN0004		
	GGAGGGAAAAGTTATCAGGCGAGTGCGTAATGGTACGATTTGGGAAGTGGCTTGGGGTGGGATTAGTTTTGGAGTACTCGCTCC	11
	GAAAAGTTATCAGGCGAGTGCGTAATGGTACGATTTGGGAAGTGGCTTGGGGTGGGATTAGTTTTGGAGTACTCGCTCC	19
	GAGTGCGTAATGGTACGATTTGGGAAGTGGCTTGGGGTGGGATTAGTTTTGGAGTACTCGCTCC ☆	3
	GAGTGCGTAATGGTACGATTTGGGAAGTGGCTTGGGGTGGGATTAGTTTTGGAGTACTC-B	57
	GAGTGCGTAATGGTACGATTTGGGAAGTGGCTTGGGGTGGGATTAGTTTTGGG	67
	GAGTGCGTAATGGTACGATTTGGGAAGTGGCTTGGGGTGGG ☆	83
	GAGTGCGTAATGGTACGATTTGGGAAGTGGCTTGGGGTGG	>1000
	ATGGTACGATTTGGGAAGTGGCTTGGGGTGGG	230
CLN0020		
	GGAGGGAAAAGTTATCAGGCCACTGCGGGGGTCTATACGTGAGGAAGAAGTGGGCAGGTCGATTAGTTTTGGAGTACTCGCTCC	45
	GAAAAGTTATCAGGCCACTGCGGGGGTCTATACGTGAGGAAGAAGTGGGCAGGTCGATTAGTTTTGGAGTACTCGCTCC	25
	CACTGCGGGGGTCTATACGTGAGGAAGAAGTGGGCAGGTCGATTAGTTTTGGAGTACTCGCTCC	68
	GGAGGGAAAAGTTATCAGGCCACTGCGGGGGTCTATACGTGAGGAAGAAGTGGGCAGGTC	40
	GAAAAGTTATCAGGCCACTGCGGGGGTCTATACGTGAGGAAGAAGTGGGCAGGTC-B	22
	CAGGCCACTGCGGGGGTCTATACGTGAGGAAGAAGTGGGCAGGTC	20
	CCACTGCGGGGGTCTATACGTGAGGAAGAAGTGGGCAGGTC ☆	68
	CACTGCGGGGGTCTATACGTGAGGAAGAAGTGGGCAGGTC	55
	CCACTGCGGGGGTCTATACGTGAGGAAGAAGTGG ☆	>1000
CLN0123		47
	GGAGGGAAAAGTTATCAGGCAGAGGGGAGGGTCGGGTATCGGCGTGTTCGGGGGATCTGCGATTAGTTTTGGAGTACTCGCTCC-B ☆	195
	AAAGTTATCAGGCAGAGGGGAGGGTCGGGTATCGGCGTGTTCGGGGGATCTGCGATTAGTTTTGGAGTACTCGCTCC	220
	TCAGGCAGAGGGGAGGGTCGGGTATCGGCGTGTTCGGGGGATCTGCGATTAGTTTTGGAGTACTCGCTCC	169
	AGAGGGGAGGGTCGGGTATCGGCGTGTTCGGGGGATCTGCGATTAGTTTTGGAGTACTCGCTCC	232
	GGAGGGAAAAGTTATCAGGCAGAGGGGAGGGTCGGGTATCGGCGTGTTCGGGGGATCTGCGATTAGTTTTGGGAGTA	83
	GGAGGGAAAAGTTATCAGGCAGAGGGGAGGGTCGGGTATCGGCGTGTTCGGGGGATCTGCGATTAGTT	68
	GGAGGGAAAAGTTATCAGGCAGAGGGGAGGGTCGGGTATCGGCGTGTTCGGGGGATCTGC	128

FIGURE 3. **Structure prediction and dot blot-based minimization.** *A*, CLN0020 structure prediction indicating nucleotides 20–53 to be essential for structure formation. Numbering indicates base numbers of the full-length aptamer. *B*, affinity alteration upon removal of C20 in CLN0020 as determined in a dot blot. *C*, dot blot minimization studies of c-Met specific CLN0003 and CLN0004 as well as CD16α specific CLN0020 and CLN0123. Aptamers could be minimized individually up to a 34-mer CLN0020 core sequence. *Asterisks* mark the truncation variants used for the design of bi-specific aptamers.

TABLE 2

Selected bi-specific aptamers (a complete list can be found in supplemental Table S3)

Construct	5′ aptamer[a]	Linker sequence	3′ aptamer	Putative linker length[b]	CD16α-6His K_D	n	c-Met-Fc K_D	n
				Å	nM		nM	
bsA3	-19CLN0020-24	GCAGGTCAAAAAAAAAAAAAAAAA	-20CLN0004-23	154	39 ± 10	3	141 ± 16	6
bsA31	-19CLN0020-24	GCAGGTCAAAAAAAAAAAAAAAAA	-20CLN0004	154	24 ± 4	4	92 ± 41	3
bsA32	-19CLN0020-31	AAAAAAAAAAAAAAA	-20CLN0004	105	33 ± 1	2	119 ± 22	3
bsA11	-19CLN0020	GCAGGTCGATTAGTTTTGGAGTACTCGCTCC	CLN0003	217	82 ± 9	2	0.16	1
bsA15	CLN0123	GATTAGTTTTGGAGTACTC	CLN0003	140	174	1	0.22	1
bsA17	-19CLN0020-24	GCAGGTC	CLN0003	49	19 ± 2	3	0.35 ± 0.09	6
bsA21	-19CLN0020-24	GCAGGTCAAAAAAAAAAAAAAAAA	CLN0003	154	19 ± 2	2	0.28 ± 0.12	3
bsA22	-19CLN0020-31	AAAAAAAAAAAAAAA	CLN0003	105	27 ± 5	2	0.24 ± 0.10	3

[a] 20CLN0020 denotes a 20-nucleotide truncation 5′ of CLN0020, CLN0020–24 designates a 24-nucleotide truncation 3′ of CLN0020, and so forth.

[b] Maximal distances bridged by nucleotide linkers were estimated from x-ray structures as described under "Experimental Procedures."

migration shift assays (EMSA; Fig. 4). All other bi-specific aptamers exhibited similar patterns (data not shown). Additional bio-layer interferometry confirmed simultaneous binding of bsA17 to c-Met-Fc and Fc-CD16α Val-158 (supplemental Fig. S13).

Serum Stability—Because further functional assays demanded measurements in the presence of serum and stability was of interest for this therapeutic concept, the serum half-life of selected radiolabeled aptamers was determined to be 9.8 (CLN0004), 14.5 (CLN0020), 6.4 (bsA3), and 20.3 h (bsA17) in freshly thawed FCS. In addition, bsA17 remained stable in PBS for 48 h (Fig. 5 and supplemental Fig. S14).

ADCC Assays—Bi-specific aptamers displaying high affinities and simultaneous binding to both target proteins as well as suitable serum stabilities were applied in functional ADCC assays. 16 suitable bi-specific aptamers were evaluated, including

ing CLN0004-derived bsA31 (probably with suitable linker but with relatively low c-Met affinity) as well as CLN0003-based bsA11, -15, -17, and -22 (sharing high c-Met affinities combined with varying linkers; supplemental Tables S3 and S4). Bi-specific aptamer bsA17 mediated cellular cytotoxicity on GTL-16 and EBC-1 cells with a similar magnitude to antibody-positive control cetuximab (Fig. 6, *A* and *B*). This effect was reduced by either aptamer or effector cell dilution (Fig. 6, *A*–*C*). In addition, blocking of aptamer binding to CD16α by the addition of competing antibody 3G8 in 20-fold excess led to a significant decrease of specific cell lysis, further supporting the proposed mode of action (Fig. 6*G*). The bsA17-related bi-specific aptamer bsA22 similarly mediated specific GTL-16 cell lysis that could be diminished by reduction of aptamer concentration or effector cell amount (Fig. 6, *E* and *F*). CLN0004-derived bsA31, showing lower c-Met affinity (92 nM), induced
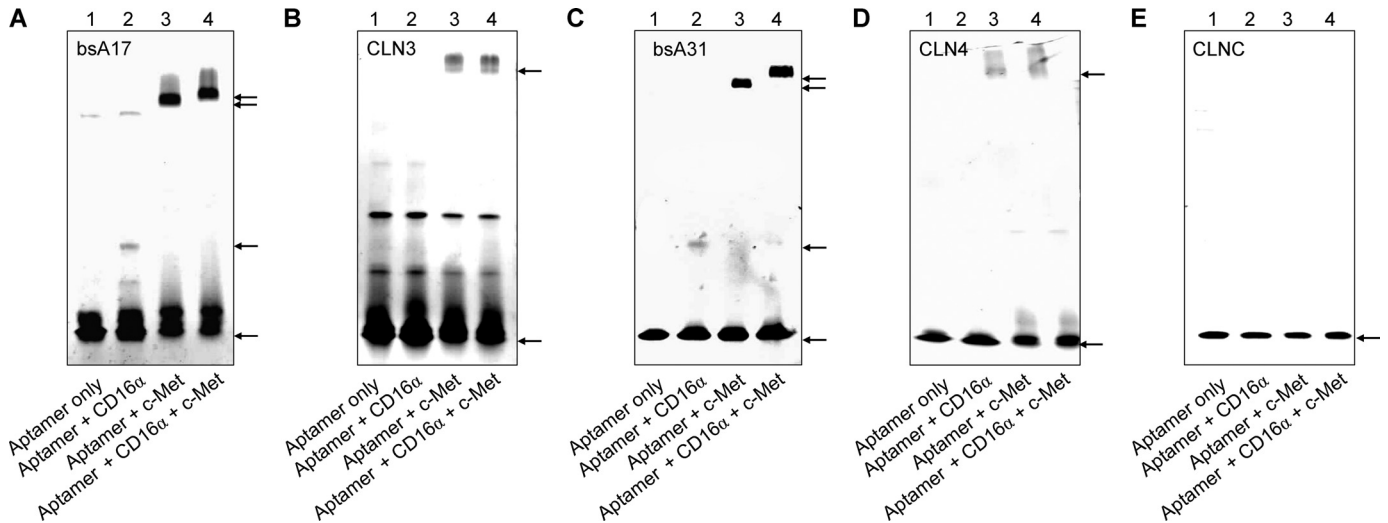
FIGURE 4. **Simultaneous binding of bi-specific aptamers bsA17 and bsA31 to CD16α and c-Met.** *A,* CLN0003-derived bsA17 exhibited binding to CD16α-6His (additional band in *lane 2*) or c-Met-Fc fusion proteins (additional band in *lane 3*). This c-Met-Fc bound aptamer band shifted again upon the addition of CD16α-6His (*lane 4*). *B,* negative control parental single aptamer CLN0003 did not show a migration shift. Additional bands in all lanes could be due to unspecific aggregation. *C* and *D,* bsA31 and original single c-Met specific aptamer CLN0004 exhibited the same pattern as in *A* and *B. E,* negative control aptamer (*CLNC*) did not bind to any protein, as expected. Application of a gradient gel and size differences between CD16α-6His and c-Met-Fc fusion protein led to differently extended migration (*lanes 2* and *3*) and an expectedly minor but clearly present migration shift upon the addition of both target proteins (from *lane 3* to *4*). *Arrows* indicate the lowest migration frontier of specific aptamer bands.
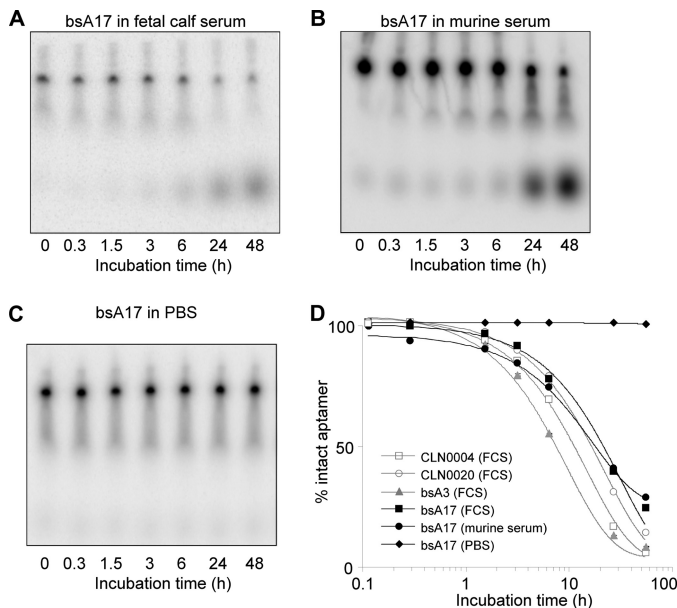
FIGURE 5. **Serum stability of major DNA aptamers.** *A* and *B,* PAGE of bsA17 after incubation in FCS or murine serum, respectively. Bands at the migration level of the 0-h sample represent intact aptamer, whereas increasing signals at lower positions depict breakdown products. *C,* degradation of bsA17 in PBS was evaluated similarly but could not be observed within 48 h. *D,* intensity values were extracted from gels, the percentage of intact aptamer was calculated, and a curve was fitted to the resulting time course. Half-lives in FCS were determined as 9.8 (CLN0004), 14.5 (CLN0020), 6.4 (bsA3), and 20.3 h (bsA17), as well as 11 h for bsA17 in murine serum. Gel raw data of stability curves of additional aptamers are not shown.

weaker but distinct cytotoxicity at higher concentrations above 100 nM (Fig. 6*H*). Bi-specific aptamer bsA15 (with lower CD16α affinity) mediated specific GTL-16 cell lysis at comparable concentrations but with lower maximal cell lysis (Fig. 6*I*). When comparing bi-specific aptamers differing mostly in linker length, only linkers of ~50–100 Å (of bsA17 and bsA22) were more suitable than longer linkers (217 Å of bsA11, Fig. 6*D*). It

must be noted that putative linker lengths were calculated based on crystal structures of other DNA aptamers, so these linker lengths were estimations only. Although a precise EC_{50} determination was not feasible with mostly qualitative data obtained, the half-effective dose of bsA17 and bsA22 was in the low two-digit nanomolar range of 1–50 nM (Fig. 6, *A, B,* and *E*). Supplemental Table S4 gives a concluding overview of analyzed bi-specific aptamers and all properties that have been characterized.

DISCUSSION

Aptamer Selection and Characterization—Both filter and cell SELEX approaches with CD16β counterselection led to the selection of CD16α specific DNA aptamers that did not bind CD16β. Although the specificity is surprising, it is in line with reported aptamers that can be highly specific (48, 49). In comparison with antibodies, CD16α specificity could prevent decoy of therapeutically applied bsA by soluble CD16β vastly present in the blood and ensure recruitment of CD16α-presenting effector cells. In addition, high affinity to both CD16α Val-158 and Phe-158 allotypes could enable a positive ADCC response in all patients, whereas in current antibody therapies, V/V allele carriers are associated with higher ADCC and improved clinical outcome than F/F patients (28, 31). Unexpectedly, aptamers that were enriched in cell SELEX and showed high CD16α affinity in dot blot assays mostly did not bind CD16α on the same cells as used for selection in flow cytometric measurements. Similarly, most filter SELEX-derived CD16α specific aptamers bound to recombinant CD16α-6His with high affinity, but not to cellular CD16α presented on recombinant Jurkat or NK cells. This could be due to disruption of their tertiary structure by binding of comparatively large streptavidin-phycoerythrin conjugates for staining purposes. Because such aptamers were probably not suitable to serve as one entity coupled to another aptamer in bi-specific constructs, optimization
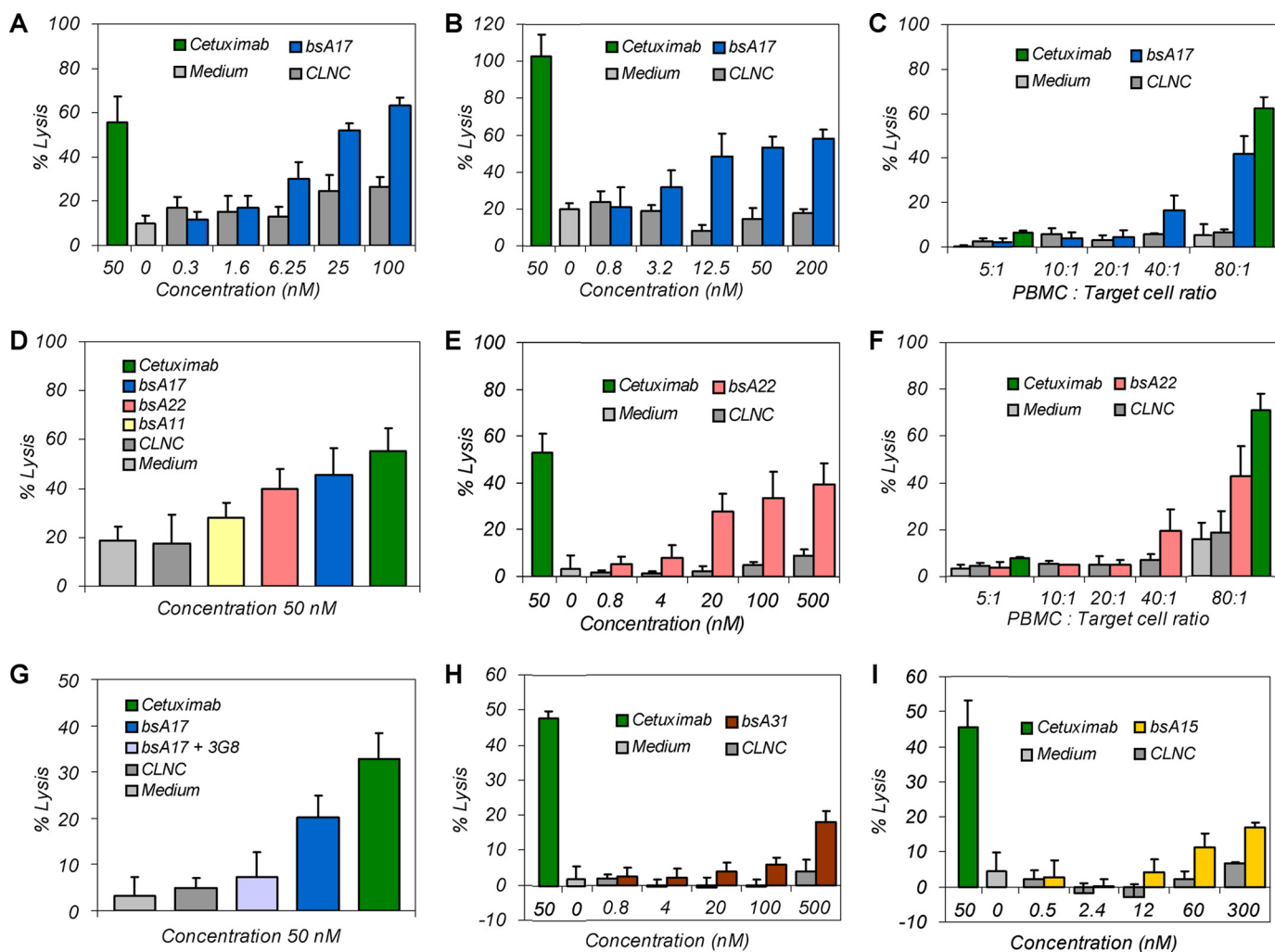
FIGURE 6. **Functional ADCC assays of bi-specific aptamers.** *A*, bi-specific aptamer bsA17-mediated specific GTL-16 cell lysis as compared with background levels of non-binding negative control aptamer (*CLNC*) and reference with medium only. *B*, similar bsA17-mediated concentration-dependent specific EBC-1 cell lysis. *C*, PBMC:target cell ratio reduction diminished cytotoxicity of both bsA17 and cetuximab at 50 nм. *D*, influence of linker lengths on bsA-mediated cell lysis. Estimated linker lengths were 49 Å for bsA17, 105 Å for bsA22 and 217 Å for bsA11. *E* and *F*, bsA22-induced specific cytotoxicity dependent on aptamer concentration and effector cell amount. *G*, the addition of 20-fold molar excess of antibody 3G8 resulted in a decrease of bsA17-mediated lysis due to inhibition of bsA17-binding to CD16α. *H*, bsA31 with lower c-Met affinity induced weaker but distinct lysis at higher concentrations. *I*, bsA15, composed of CLN0123 as a lower affinity CD16α binding entity, mediated weak but significant cytotoxicity as well. GTL-16 cells were applied in all measurements, except for *B*. Maximal lysis varied between individual experiments due to donor and CD16α allotype dependence. ADCC assays were performed 5 times with $n = 4$ (*A*), 4 times with $n = 4$ (*B*), 3 times with $n = 3$ (*C*), 3 times with $n = 9$ (*D*), 4 times with $n = 4$ (*E*), 1 time with $n = 3$ (*F*), 3 times with $n = 9$ (*G*), 2 times with $n = 4$ (*H*), and 1 time with $n = 4$ (*I*), and representative measurements are shown as mean ± S.D.

of the detection method (*e.g.* switching to direct dye labeling) was not performed.

Selected c-Met specific aptamers exhibited desirable properties such as high affinity and clear cellular binding (Fig. 2) but recognized the same epitope on c-Met (supplemental Fig. S11), impeding examination of epitope dependence for cytotoxic efficacy (*cf.* Ref. 50). This work represents the first description of DNA aptamers that show high specificity and affinity to c-Met or CD16α.

Design of Bi-specific Aptamers—The design of bi-specific aptamers included the development of linkers to approximately match the distance between complementarity-determining regions and the Fc binding domain in whole antibodies. The rationale was mimicking antibody architecture to improve the chance of enabling a similar cytotoxic effect. Mostly, linkers were designed based on the respective full-length sequences because minimization studies had shown that these sequences

were not essential and did not interfere with high affinity binding. Additionally, 15-deoxyadenosine linkers were used as described by Müller *et al.* (46). Most linkers enabled both original affinity and simultaneous target protein binding (Table 2, Fig. 4, and supplemental Table S4). Calculated linker lengths were based on nucleotide distances in single-stranded portions of DNA aptamer crystal structures and consequently represented an estimate only. Coupling of bi-specific aptamers was achieved by complete synthesis rather than hybridization to obtain more uniform bi-specific aptamers.

Serum half-lives were determined in murine and fetal calf serum to be 6.4–20.3 h (Fig. 5). Stabilities were in accordance with comparable studies of DNA aptamer degradation in human serum and plasma, reporting strongly varying half-lives from several minutes to 42 h (51–53). Differences may reflect diverse applied methods (51, 54) or a strong sequence dependence of nuclease degradation (55) including a rigid structure

versus exposed termini (5). In addition to high affinity simultaneous binding, bsA serum stabilities provided clear evidence of the suitability for functional evaluation.

Functional Analyses—Aptamer-mediated cellular cytotoxicity was dependent on the concentration of bi-specific aptamers and the amount of applied effector cells. Reduced lysis upon CD16 binding blocking by 3G8 provided proof for the suggested mode of action. Specific cytotoxicity was demonstrated for independent human gastric and lung cancer cell lines and determined 3–6 times in independent experiments applying effector cells of different blood donors. Taken together, these results validate that bi-specific aptamers can mediate specific cellular cytotoxicity. Maximal specific cell lysis (Fig. 6) was similar to comparable bi-specific scFv formats (35, 56, 57) and therapeutical antibodies (58). Activation with IL-2 or longer incubation could have further increased maximal lysis (59, 60). Note that the actual effector:target cell (E:T) ratio was ~8:1 when applying 80:1 PBMC:target cells (32). Because ADCC-mediating c-Met specific antibodies R13 and R28 (61) were not available for comparative studies, EGF receptor-specific cetuximab was used as a qualitative antibody-positive control and as an indicator for a valid experimental setup including *e.g.* suitable NK cell reactivity.

In quantitative comparison with the potency reported for the two c-Met specific antibodies R13 and R28 of 60 nM EC_{50} (when synergistically applied (61)), half-effective concentrations were lower for individually applied bsA17 or bsA22 (10–50 nM; Fig. 6). Other published c-Met antibody therapeutics comprise only Fab fragments (11) or *Escherichia coli*-produced monovalent antibodies (MetMAb (12)) that do not induce cellular cytotoxicity. Therapeutic "enhanced ADCC" antibodies target other surface proteins and exhibit EC_{50} values in a low ng/ml range translating to low picomolar concentrations (58). CD16α-targeting bi-specific scFv formats that are comparable with bsAs described herein show half-maximum effective doses at low nanomolar (62) to three-digit picomolar concentrations (45, 57), whereas similar constructs as trivalent bi-specific triple bodies mediate ADCC with low picomolar EC_{50} values (35, 56). Finally, CD3 specific T cell recruiting BiTEs exhibit half-maximum effective doses partly below 1 ng/ml, which equals low picomolar to femtomolar concentrations (59, 60). Due to target protein dependence of ADCC, direct comparison of bi-specific aptamers is only feasible to c-Met antibodies applied to GTL-16 cells, and single bi-specific aptamers bsA17 or bsA22 alone exhibit a higher potency than synergistically applied c-Met antibodies R13 and R28 (61).

Cytotoxicity was mediated by high affinity bsAs containing linkers that maximally bridge ~49–154 Å, a distance similar to ~65 Å in antibodies. In accordance to these findings, effective bi-specific scFv molecules contain Gly-Ser linkers bridging similar distances (*e.g.* 110 Å in Ref. 35). Decreased cytolytic efficacies were observed with increasing linker lengths, and linkers with putative separation distances over ~200 Å did not elicit significant cytotoxicity, regardless of high affinities to both target proteins (*e.g.* bsA11 in Fig. 6*D*). This indicates the importance of the spatial distance for enabling cellular cytotoxicity (as evaluated in another way by Bluemel *et al.* in Ref. 50).

Perspective—The bi-specific aptamers described herein exhibit affinities similar to certain BiTEs with three-digit picomolar to low nanomolar tumor antigen binding and medium affinity effector specific antigen binding (63). These similar characteristics point out that bi-specific aptamers could induce serial killing of NK cells (cf. 64). However, the efficacy of BiTEs clearly supersedes that of the first generation bi-specific aptamers reported herein. Relocalization of cytotoxic T cells instead of NK cells by targeting CD3 instead of CD16 could potentially increase the efficacy of bi-specific aptamers. In this study, c-Met was used to bring NK cells into close proximity of tumor cells to trigger ADCC, but the application range of bi-specific aptamers could be broadened by facile exchange of the tumor-specific portion targeting further tumor markers such as the validated targets EpCAM or EGF receptor.

Future work could focus on *in vivo* evaluations using xenograft mouse models expressing human CD16 receptors (65, 66). Despite positive results in functional cellular assays, issues of serum stability and poor pharmacokinetics remain to be solved. Stability can be further improved, *e.g.* by usage of modified nucleotides with substituted 2′ residues. Suitable 2′-hydroxy-purine 2′-fluoro-pyrimidine oligonucleotide and 2′-methoxy-purine 2′-fluoro-pyrimidine oligonucleotide aptamers (67), sharing all essential characteristics with the successfully employed DNA aptamer CLN0020, are already available (supplemental Figs. S15–S17). Renal clearance could be reduced by aptamer coupling to PEG (68), hydroxyethyl starch, or other glycosylation (69, 70). In a more elegant approach, neonatal Fc receptor (FcRn)-mediated recycling of antibodies (71) could be mimicked by additional coupling of aptamers binding to the neonatal Fc receptor FcRn at pH 6 but not at pH 7.4.[3] In contrast to antibodies, aptamers as single binding entities possess the property of binding tumor-specific surface receptors without the risk of activation (11). Bi-specific aptamers optimized in such ways could mimic most eligible features of comparable therapeutic antibody approaches but exceed them, for example, with uniform and cost-effective synthesis as well as a proposed absence of immunogenicity (13, 73).

So far, work was published on linkage of aptamers that aimed at delivery of payloads (8, 74), an affinity increase by avidity, and a stronger receptor (75) or enzyme inhibition (76–78). Furthermore, two copies of RNA aptamers were assembled on an oligonucleotide-based scaffold to induce receptor activation (79), and with it, T cell co-stimulation that led to tumor growth inhibition in mice (6). Bi-specific aptamers have also been developed to capture different ligands in diagnostic applications (80). To our knowledge, the work presented herein describes for the first time the gain of a tumor-effective function of two distinct binding entities by linkage into a bi-specific aptamer mediating tumor cell lysis. Bi-specific aptamers represent a suitable starting concept for the development of stable, nucleotide-based therapeutics to mediate lysis of c-Met-positive tumors. A facile exchange of the tumor-specific entity could broaden the approach to treatment of further cancer types, thereby opening new avenues for tumor therapy.

---

[3] R. Günther, unpublished results.

Bi-specific Aptamers Mediating Tumor Cell Lysis

REFERENCES

1. Ruckman, J., Green, L. S., Beeson, J., Waugh, S., Gillette, W. L., Henninger, D. D., Claesson-Welsh, L., and Janjić, N. (1998) *J. Biol. Chem.* **273,** 20556–20567
2. Sazani, P. L., Larralde, R., and Szostak, J. W. (2004) *J. Am. Chem. Soc.* **126,** 8370–8371
3. Ellington, A. D., and Szostak, J. W. (1990) *Nature* **346,** 818–822
4. Tuerk, C., and Gold, L. (1990) *Science* **249,** 505–510
5. Di Giusto, D. A., Knox, S. M., Lai, Y., Tyrelle, G. D., Aung, M. T., and King, G. C. (2006) *Chembiochem* **7,** 535–544
6. McNamara, J. O., Kolonias, D., Pastor, F., Mittler, R. S., Chen, L., Giangrande, P. H., Sullenger, B., and Gilboa, E. (2008) *J. Clin. Invest.* **118,** 376–386
7. Dassie, J. P., Liu, X. Y., Thomas, G. S., Whitaker, R. M., Thiel, K. W., Stockdale, K. R., Meyerholz, D. K., McCaffrey, A. P., McNamara, J. O., 2nd, and Giangrande, P. H. (2009) *Nat. Biotechnol.* **27,** 839–849
8. Zhou, J., Swiderski, P., Li, H., Zhang, J., Neff, C. P., Akkina, R., and Rossi, J. J. (2009) *Nucleic. Acids Res.* **37,** 3094–3109
9. Orava, E. W., Cicmil, N., and Gariépy, J. (2010) *Biochim. Biophys. Acta* **1798,** 2190–2200
10. Aarden, L., Ruuls, S. R., and Wolbink, G. (2008) *Curr. Opin. Immunol.* **20,** 431–435
11. Pacchiana, G., Chiriaco, C., Stella, M. C., Petronzelli, F., De Santis, R., Galluzzo, M., Carminati, P., Comoglio, P. M., Michieli, P., and Vigna, E. (2010) *J. Biol. Chem.* **285,** 36149–36157
12. Jin, H., Yang, R., Zheng, Z., Romero, M., Ross, J., Bou-Reslan, H., Carano, R. A., Kasman, I., Mai, E., Young, J., Zha, J., Zhang, Z., Ross, S., Schwall, R., Colbern, G., and Merchant, M. (2008) *Cancer Res.* **68,** 4360–4368
13. White, R. R., Sullenger, B. A., and Rusconi, C. P. (2000) *J. Clin. Invest.* **106,** 929–934
14. Que-Gewirth, N. S., and Sullenger, B. A. (2007) *Gene Ther.* **14,** 283–291
15. Bates, P. J., Choi, E. W., and Nayak, L. V. (2009) *Methods Mol. Biol.* **542,** 379–392
16. Keefe, A. D., Pai, S., and Ellington, A. (2010) *Nat. Rev. Drug. Discov.* **9,** 537–550
17. Zompi, S., and Colucci, F. (2005) *Immunol. Lett* **97,** 31–39
18. Sliwkowski, M. X., Lofgren, J. A., Lewis, G. D., Hotaling, T. E., Fendly, B. M., and Fox, J. A. (1999) *Semin. Oncol.* **26,** 60–70
19. Desjarlais, J. R., Lazar, G. A., Zhukovsky, E. A., and Chu, S. Y. (2007) *Drug Discov. Today* **12,** 898–910
20. Farag, S. S., VanDeusen, J. B., Fehniger, T. A., and Caligiuri, M. A. (2003) *Int. J. Hematol.* **78,** 7–17
21. Kim, S., Iizuka, K., Aguila, H. L., Weissman, I. L., and Yokoyama, W. M. (2000) *Proc. Natl. Acad. Sci. U.S.A.* **97,** 2731–2736
22. Roda, J. M., Parihar, R., Magro, C., Nuovo, G. J., Tridandapani, S., and Carson, W. E., 3rd (2006) *Cancer Res.* **66,** 517–526
23. Nimmerjahn, F., and Ravetch, J. V. (2006) *Immunity* **24,** 19–28
24. Bruhns, P., Iannascoli, B., England, P., Mancardi, D. A., Fernandez, N., Jorieux, S., and Daëron, M. (2009) *Blood* **113,** 3716–3725
25. Harrison, D., Phillips, J. H., and Lanier, L. L. (1991) *J. Immunol.* **147,** 3459–3465
26. Li, P., Jiang, N., Nagarajan, S., Wohlhueter, R., Selvaraj, P., and Zhu, C. (2007) *J. Biol. Chem.* **282,** 6210–6221
27. Huizinga, T. W., de Haas, M., van Oers, M. H., Kleijer, M., Vilé, H., van der Wouw, P. A., Moulijn, A., van Weezel, H., Roos, D., and von dem Borne, A. E. (1994) *Br. J. Haematol.* **87,** 459–463
28. Cartron, G., Dacheux, L., Salles, G., Solal-Celigny, P., Bardos, P., Colombat, P., and Watier, H. (2002) *Blood* **99,** 754–758
29. López-Albaitero, A., Lee, S. C., Morgan, S., Grandis, J. R., Gooding, W. E., Ferrone, S., and Ferris, R. L. (2009) *Cancer Immunol. Immunother.* **58,** 1853–1864
30. Cui, Z., Willingham, M. C., Hicks, A. M., Alexander-Miller, M. A., Howard, T. D., Hawkins, G. A., Miller, M. S., Weir, H. M., Du, W., and DeLong, C. J. (2003) *Proc. Natl. Acad. Sci. U.S.A.* **100,** 6682–6687
31. Taylor, R. J., Chan, S. L., Wood, A., Voskens, C. J., Wolf, J. S., Lin, W., Chapoval, A., Schulze, D. H., Tian, G., and Strome, S. E. (2009) *Cancer Immunol. Immunother.* **58,** 997–1006
32. Wallace, M. E., and Smyth, M. J. (2005) *Springer Semin. Immunopathol.* **27,** 49–64
33. Arndt, M. A., Krauss, J., Kipriyanov, S. M., Pfreundschuh, M., and Little, M. (1999) *Blood* **94,** 2562–2568
34. McCall, A. M., Adams, G. P., Amoroso, A. R., Nielsen, U. B., Zhang, L., Horak, E., Simmons, H., Schier, R., Marks, J. D., and Weiner, L. M. (1999) *Mol. Immunol.* **36,** 433–445
35. Singer, H., Kellner, C., Lanig, H., Aigner, M., Stockmeyer, B., Oduncu, F., Schwemmlein, M., Stein, C., Mentz, K., Mackensen, A., and Fey, G. H. (2010) *J. Immunother.* **33,** 599–608
36. Baeuerle, P. A., and Reinhardt, C. (2009) *Cancer Res.* **69,** 4941–4944
37. Eder, J. P., Vande Woude, G. F., Boerner, S. A., and LoRusso, P. M. (2009) *Clin. Cancer Res.* **15,** 2207–2214
38. Tsarfaty, I., Rong, S., Resau, J. H., Rulong, S., da Silva, P. P., and Vande Woude, G. F. (1994) *Science* **263,** 98–101
39. Gentile, A., Trusolino, L., and Comoglio, P. M. (2008) *Cancer Metastasis Rev.* **27,** 85–94
40. Bladt, F., Riethmacher, D., Isenmann, S., Aguzzi, A., and Birchmeier, C. (1995) *Nature* **376,** 768–771
41. Stellrecht, C. M., and Gandhi, V. (2009) *Cancer Lett* **280,** 1–14
42. Takayama, H., LaRochelle, W. J., Sharp, R., Otsuka, T., Kriebel, P., Anver, M., Aaronson, S. A., and Merlino, G. (1997) *Proc. Natl. Acad. Sci. U.S.A.* **94,** 701–706
43. Tsang, J., and Joyce, G. F. (1996) *J. Mol. Biol.* **262,** 31–42
44. Zuker, M. (2003) *Nucleic Acids Res.* **31,** 3406–3415
45. Bruenke, J., Fischer, B., Barbin, K., Schreiter, K., Wachter, Y., Mahr, K., Titgemeyer, F., Niederweis, M., Peipp, M., Zunino, S. J., Repp, R., Valerius, T., and Fey, G. H. (2004) *Br. J. Haematol.* **125,** 167–179
46. Müller, J., Wulffen, B., Pötzsch, B., and Mayer, G. (2007) *Chembiochem* **8,** 2223–2226
47. Radaev, S., Motyka, S., Fridman, W. H., Sautes-Fridman, C., and Sun, P. D. (2001) *J. Biol. Chem.,* **276,** 16469–16477
48. Jenison, R. D., Gill, S. C., Pardi, A., and Polisky, B. (1994) *Science* **263,** 1425–1429
49. Shangguan, D., Li, Y., Tang, Z., Cao, Z. C., Chen, H. W., Mallikaratchy, P., Sefah, K., Yang, C. J., and Tan, W. (2006) *Proc. Natl. Acad. Sci. U.S.A.* **103,** 11838–11843
50. Bluemel, C., Hausmann, S., Fluhr, P., Sriskandarajah, M., Stallcup, W. B., Baeuerle, P. A., and Kufer, P. (2010) *Cancer Immunol. Immunother.* **59,** 1197–1209
51. Di Giusto, D. A., and King, G. C. (2004) *J. Biol. Chem.* **279,** 46483–46489
52. Schmidt, K. S., Borkowski, S., Kurreck, J., Stephens, A. W., Bald, R., Hecht, M., Friebe, M., Dinkelborg, L., and Erdmann, V. A. (2004) *Nucleic Acids Res.* **32,** 5757–5765
53. Peng, C. G., and Damha, M. J. (2007) *Nucleic Acids Res.* **35,** 4977–4988
54. Shaw, J. P., Fishback, J. A., Cundy, K. C., and Lee, W. A. (1995) *Pharm. Res.* **12,** 1937–1942
55. Choi, E. W., Nayak, L. V., and Bates, P. J. (2010) *Nucleic Acids Res.* **38,** 1623–1635
56. Kellner, C., Bruenke, J., Stieglmaier, J., Schwemmlein, M., Schwenkert, M., Singer, H., Mentz, K., Peipp, M., Lang, P., Oduncu, F., Stockmeyer, B., and Fey, G. H. (2008) *J. Immunother.* **31,** 871–884
57. Kügler, M., Stein, C., Kellner, C., Mentz, K., Saul, D., Schwenkert, M., Schubert, I., Singer, H., Oduncu, F., Stockmeyer, B., Mackensen, A., and Fey, G. H. (2010) *Br. J. Haematol.* **150,** 574–586
58. Lazar, G. A., Dang, W., Karki, S., Vafa, O., Peng, J. S., Hyun, L., Chan, C., Chung, H. S., Eivazi, A., Yoder, S. C., Vielmetter, J., Carmichael, D. F., Hayes, R. J., and Dahiyat, B. I. (2006) *Proc. Natl. Acad. Sci. U.S.A.* **103,** 4005–4010
59. Mack, M., Riethmüller, G., and Kufer, P. (1995) *Proc. Natl. Acad. Sci. U.S.A.* **92,** 7021–7025
60. Brischwein, K., Schlereth, B., Guller, B., Steiger, C., Wolf, A., Lutterbuese,

R., Offner, S., Locher, M., Urbig, T., Raum, T., Kleindienst, P., Wimberger, P., Kimmig, R., Fichtner, I., Kufer, P., Hofmeister, R., da Silva, A. J., and Baeuerle, P. A. (2006) *Mol. Immunol.* **43,** 1129–1143

61. van der Horst, E. H., Chinn, L., Wang, M., Velilla, T., Tran, H., Madrona, Y., Lam, A., Ji, M., Hoey, T. C., and Sato, A. K. (2009) *Neoplasia* **11,** 355–364

62. Kipriyanov, S. M., Cochlovius, B., Schäfer, H. J., Moldenhauer, G., Bähre, A., Le Gall, F., Knackmuss, S., and Little, M. (2002) *J. Immunol.* **169,** 137–144

63. Baeuerle, P. A., Kufer, P., and Lutterbüse, R. (2003) *Curr. Opin. Mol. Ther.* **5,** 413–419

64. Hoffmann, P., Hofmeister, R., Brischwein, K., Brandl, C., Crommer, S., Bargou, R., Itin, C., Prang, N., and Baeuerle, P. A. (2005) *Int. J. Cancer* **115,** 98–104

65. Li, M., Wirthmueller, U., and Ravetch, J. V. (1996) *J. Exp. Med.* **183,** 1259–1263

66. Nimmerjahn, F., and Ravetch, J. V. (2008) *Nat. Rev. Immunol.* **8,** 34–47

67. Keefe, A. D., and Cload, S. T. (2008) *Curr. Opin. Chem. Biol.* **12,** 448–456

68. Pendergrast, P. S., Marsh, H. N., Grate, D., Healy, J. M., and Stanton, M. (2005) *J. Biomol. Tech.* **16,** 224–234

69. Kontermann, R. E. (2009) *BioDrugs* **23,** 93–109

70. Constantinou, A., Chen, C., and Deonarain, M. P. (2010) *Biotechnol. Lett* **32,** 609–622

71. Roopenian, D. C., and Akilesh, S. (2007) *Nat. Rev. Immunol.* **7,** 715–725

72. Deleted in proof

73. Kaur, G., and Roy, I. (2008) *Expert. Opin. Investig. Drugs* **17,** 43–60

74. Chu, T. C., Twu, K. Y., Ellington, A. D., and Levy, M. (2006) *Nucleic Acids Res.* **34,** e73

75. Santulli-Marotto, S., Nair, S. K., Rusconi, C., Sullenger, B., and Gilboa, E. (2003) *Cancer Res.* **63,** 7483–7489

76. Kim, Y., Cao, Z., and Tan, W. (2008) *Proc. Natl. Acad. Sci. U.S.A.* **105,** 5664–5669

77. Michalowski, D., Chitima-Matsiga, R., Held, D. M., and Burke, D. H. (2008) *Nucleic Acids Res.* **36,** 7124–7135

78. Müller, J., Freitag, D., Mayer, G., and Pötzsch, B. (2008) *J. Thromb. Haemost.* **6,** 2105–2112

79. Dollins, C. M., Nair, S., Boczkowski, D., Lee, J., Layzer, J. M., Gilboa, E., and Sullenger, B. A. (2008) *Chem. Biol.* **15,** 675–682

80. Tahiri-Alaoui, A., Frigotto, L., Manville, N., Ibrahim, J., Romby, P., and James, W. (2002) *Nucleic. Acids Res.* **30,** e45

81. Dang, C., and Jayasena, S. D. (1996) *J. Mol. Biol.* **264,** 268–278